



Short communication

Electrochemical reduction of CO₂ at Pb- and Sn-electrodes in a fixed-bed reactor in aqueous K₂CO₃ and KHCO₃ media

F. KÖLELİ^{1,*}, T. ATILAN¹, N. PALAMUT¹, A.M. GIZIR¹, R. AYDIN¹ and C.H. HAMANN²

¹Mersin University, Faculty of Sciences, Department of Chemistry, Mersin-Turkey

²Universität Oldenburg, Fachbereich Chemie, Postfach 25 03, D-26111 Oldenburg, Germany

(*author for correspondence, fax: +90 3243610046, e-mail: fkoleli@mersin.edu.tr)

Received 18 March 2002; accepted in revised form 2 January 2003

Key words: carbondioxide reduction, fixed-bed reactor, formic acid production, granule electrodes, lead and tin electrodes

1. Introduction

Energy-related activities, industrial processes, land-use change and waste combustion are the main sources of carbon dioxide increase in the atmosphere causing enhancement of the greenhouse effect. The reduction of CO₂ has thus become an important topic in electrochemistry. In electrochemical processes, the products obtained via reduction depend on the electrode material, electrode type (i.e., smooth metal, gas diffusion set-ups), solvent (aqueous, nonaqueous), supporting electrolyte and some form of reaction assistance (mediators, irradiation, ultrasonics) [1–16]. Products reported, for instance, are CO, HCOOH, CH₄, C₂H₄, C₂H₆, (CO₂)₂²⁻, MeOH, EtOH and even (CH₃)₂CO. These originate either as main products or, more frequently, as mixtures. For example, Hg, In, Pb or Sn electrodes are used for the cathodic reduction of CO₂ and the product detected in aqueous medium is only formic acid [1, 4–7]. Some metals, such as Pb, Tl and Hg, give oxalic acid as main product in aprotic medium [1, 5].

However, most of the afore-mentioned studies were conducted in divided H-cells with metal plate electrodes. In the present study we attempted to reduce CO₂ at Pb and Sn granules in an undivided fixed-bed reactor. The aim was to extend the electrode surface as much as possible within a relatively small electrochemical cell volume to reduce CO₂ selectively with high faradaic efficiencies to organic compounds. Reviews including proven or suggested reaction paths were given by Kaune [17] and recently by Tryk and Fujishima [18].

2. Experimental details

2.1. Cell construction and electrode preparation

The fixed-bed reactor used consists of a glass cell of 250 mm in height and 56 mm in diameter with an electrolyte volume of 100 mL and is illustrated in

Figure 1. A glass frit (G1) and a gas inlet were placed at the bottom of the cell. The thickness of the fixed-bed was about 20 mm. Pb-granules of 1 mm diameter yield a total bed surface of 148 cm². A surface area of 345 cm² was obtained by using Sn-granules of 3 mm diameter. A platinum counter electrode (6 cm² surface area) was placed directly above the electrode bed. Gas outlet, a thermometer and the mounting for reference electrode were placed at the top of the cell. A saturated calomel electrode (SCE) was used throughout the measurements. Prior to each electrolysis, Pb- and Sn-granules (Merck, 99.99%) were activated electrochemically for 2 h at –2.5 V vs SCE. After activation, the granules showed their characteristic shiny metallic colour.

2.2. Electrolyses and analytics

Electrolyses at Pb and Sn were carried out using freshly prepared 0.1 M aqueous K₂CO₃ and 0.5 M KHCO₃, made from p.a. grade chemicals (Merck) and distilled water (conductivity 1.8 μS cm⁻¹). CO₂ was bubbled through the fixed-bed and through the solution at a constant rate of 6 mL min⁻¹, allowing a saturation period of one hour before starting the electrolyses. All experiments were carried out under control potential (potentiometer PAR model 362) at five different cell voltages of –4, –5, –6, –7 and –8 V, where the corresponding electrode potentials varied depending on electrode material and electrolyte. For Pb in K₂CO₃ supporting electrolyte, the electrode potentials were –1.5, –1.8, –2.0, –2.15 and –2.25 V vs SCE, and for Sn in KHCO₃ the electrode potentials were –1.5, –1.7, –1.85, –1.95 and –2.05 V vs SCE, respectively. 5 mL samples were taken from the cell after electrolysis times of 30, 60, 90 and 120 min and their product analyses were carried out by HPLC (Perkin Elmer LC 200, ODS-18 column) and GC (Hewlett-Packard 6890, TCD, FID, Porapac Q and QS columns). The results were quite reproducible.

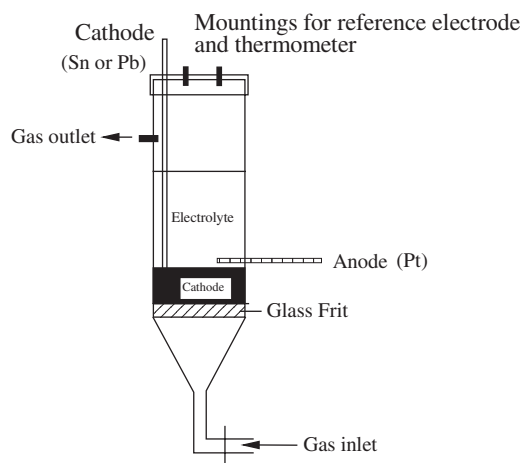


Fig. 1. Electrochemical fixed-bed reactor (schematic).

3. Results and discussion

3.1. CO_2 reduction on Pb electrode in 0.1 M aqueous K_2CO_3

Experimental results obtained from CO_2 reduction on Pb in K_2CO_3 are presented in Figure 2. During the CO_2

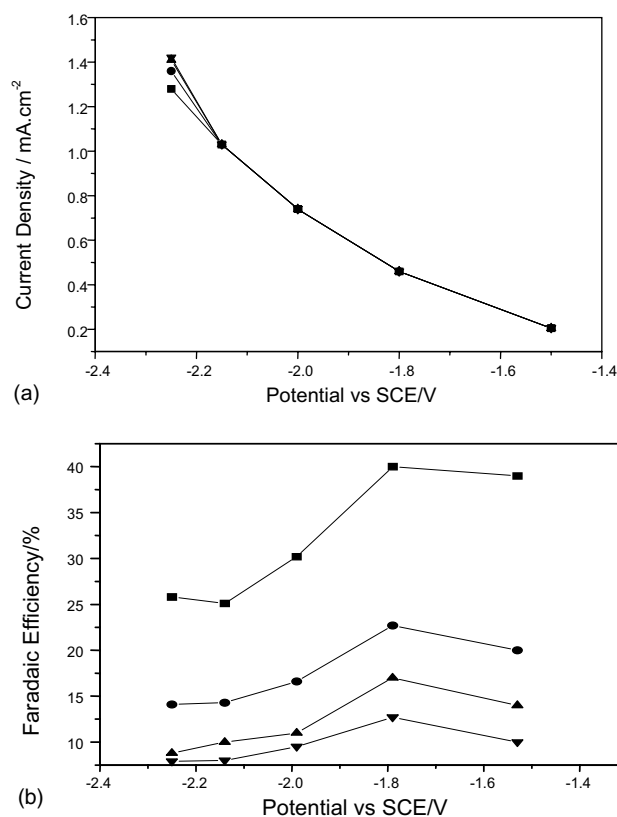


Fig. 2. (a) The current density–potential diagram of CO_2 reduction on Pb electrode at various time periods. (b) Faradaic current efficiency–potential diagram for formic acid formation on Pb electrode at different time intervals (0.1 M K_2CO_3 , pH 7.40). Key: (■) 30, (●) 60, (▲) 90 and (▼) 120 min.

reduction, formic acid was detected as the only hydrocarbon produced at negative potentials between -1.5 to -2.3 V vs SCE in aqueous solution (Figure 2(b)). Under these electrolysis conditions, no other products were detected. At more positive potentials than about -2.1 V vs SCE, the current density showed no time dependence; however, at more negative potential values, there was a slight increase with time. The more negative the potential employed, the more hydrogen evolution within the fixed-bed was observed. The highest concentration of HCOOH was found after 2 h of electrolysis time (2.2 mmol L^{-1}) at -2.2 V vs SCE.

Figure 2(b) shows the faradaic efficiency–potential diagrams for HCOOH formation with electrolysis time as a parameter. The current efficiencies reach a maximum at moderate negative potentials independent of electrolysis time and decrease at more negative potentials. This can easily be explained by increasing competitive H_2 evolution in this region.

3.2. CO_2 reduction on Pb and on Sn in 0.5 M KHCO_3

The systems Pb/ KHCO_3 and Sn/ KHCO_3 showed similar behaviour, concerning products, potential and time. Current densities and faradaic efficiencies were relatively higher in 0.5 M KHCO_3 than in 0.1 M K_2CO_3 on Pb granules, compared to Sn in both cases.

In conclusion, the system Pb/ KHCO_3 gives the best results. Table 1 presents the individual data for electrolysis times of 30 and 120 min.

3.3. Formic acid electrolyses

The faradaic efficiency decreased with electrolysis time, while potential and current density remained unchanged. This indicated formic acid consumption during electrolysis. Hence, electrolysis control tests were performed in 0.1 M K_2CO_3 and 0.5 M KHCO_3 at various electrode potentials of -1.6 , -1.8 , -2.0 and -2.2 V vs SCE with an initial HCOOH concentration of 8.7 mmol L^{-1} to determine whether or not oxidation of the products on the Pt-anode (counter electrode) occurred. As a result of this investigation, up to 11% of HCOOH was found to be oxidized in 0.1 M K_2CO_3 whereas the amount in 0.5 M KHCO_3 was considerably lower (6.0–6.5%).

3.4. Comparison with literature data

Table 2 summarizes CO_2 reduction experiments and their results as described in the literature for Pb and Sn electrodes. All experiments were carried out under ambient conditions in divided cells with metal plate electrodes, unless otherwise stated. In [2, 4, 6, 7] electrolysis times were not reported; only Hori [2] mentioned a constant current density of 5 mA cm^{-2} .

Compared to the literature values, we obtained reasonable results with respect to the current efficiencies and the overpotential values applied. However, the

Table 1. Experimental results for HCOOH formation using different electrolyte/electrode systems at ambient temperature and pressure conditions

(a) After 30 min*

Potential vs SCE/V	Current density /mA cm ⁻²				Faradaic efficiency /%			
	0.1 M K ₂ CO ₃		0.5 M KHCO ₃		0.1 M K ₂ CO ₃		0.5 M KHCO ₃	
	Pb	Sn	Pb	Sn	Pb	Sn	Pb	Sn
-1.50	0.21	–	0.79	0.25	39.0	–	90.0	74.0
-1.60	0.29	0.13	0.96	0.35	39.5	27	80.0	66.0
-1.70	0.38	0.20	1.13	0.54	39.7	29.5	74.0	62.0
-1.80	0.47	0.26	1.41	0.80	40.0	23.5	65.0	68.0
-1.90	0.63	0.42	1.72	0.90	35.0	16.5	53.0	60.0
-2.00	0.75	0.55	2.71	1.18	30.2	14.2	47.0	47.0
-2.10	0.95	0.60	3.56	1.64	27.1	11.0	45.0	29.0
-2.20	1.31	0.76	–	–	26.0	6.0	–	–

(b) After 120 min*

-1.50	0.21	–	0.79	0.03	10.0	–	30.0	20.0
-1.60	0.29	0.03	0.90	0.07	11.0	16.0	25.5	26.5
-1.70	0.41	0.04	1.18	0.11	12.0	16.5	20.5	31.0
-1.80	0.51	0.06	1.49	0.16	12.5	16.0	20.0	25.0
-1.90	0.64	0.08	1.90	0.21	11.5	15.0	20.5	21.5
-2.00	0.77	0.10	2.82	0.28	9.5	13.0	17.0	20.0
-2.10	0.92	0.11	4.36	0.36	8.0	10.5	18.0	20.0
-2.20	1.44	0.14	–	–	7.0	8.0	–	–

Table 2. CO₂ reduction data from the literature

Authors	Electrode material	Electrolyte	Electrolysis potential /V vs SCE	Product	Faradaic efficiency /%
Azuma et al. [6]	Pb	KHCO ₃	-2.20	Formic acid	16.5
	Sn				28.5
Ikeda et al. [4]	Pb	0.1 M TEAP	-2.00	Formic acid	72.9
	Sn				67.5
Hori et al. [2]	Pb	KHCO ₃	-1.62	Formic acid	72.5–88.8
	Sn		-1.40		65.0–79.9
Azuma et al. [7]	Pb	KHCO ₃	-2.20	Formic acid and others	3.8 at 2 °C
			-1.80		16.7 at 0 °C
			-2.00		16.5 at 0 °C

current densities are insufficiently high for a conventional process using the present system.

A comparison between Tables 1 and 2 shows clearly that data obtained on plate electrodes can be reproduced at fixed beds, with a resulting enhancement in the space-time yield.

4. Conclusions

The electrochemical reduction of CO₂ on Pb and Sn electrodes in aqueous KHCO₃ and K₂CO₃ electrolyte in a fixed-bed reactor was studied. Formic acid was detected as a predominant product in the working potential ranges for both electrodes. The highest current efficiency for formic acid production obtained in bicarbonate solution after 30 min at -1.5 V vs SCE was found to be 95% for Pb, and current densities up to

approximately 4.4 mA cm⁻² were achieved during CO₂ reduction.

Acknowledgements

The authors thank Mersin University Research Foundation and The Turkish Scientific Research Council (TÜBİTAK, TBAG-2007) for financial support of this work.

References

1. M. Jitaru, D.A. Lowy, M. Toma, B.C. Toma and L. Oniciu, *J. Appl. Electrochem.* **27** (1997) 875.
2. Y. Hori, K. Kikuchi and S. Suzuki, *Chem. Lett.* (1985) 1695.
3. Yu.B. Vasiliev, V.S. Bagotzky, N.V. Osetrova, O.A. Khazova and N.A. Mayorova, *J. Electroanal. Chem.* **189** (1985) 271.

4. S. Ikeda, T. Takagi and K. Ito, *Bull. Chem. Soc. Jpn.* **60** (1987) 2517.
5. G.Z. Kyriacou and A.K. Anagnostopoulos, *J. Appl. Electrochem.* **23** (1993) 483.
6. M. Azuma, K. Hashimoto, M. Hiramoto, M. Watanabe and T. Sakata, *J. Electrochem. Soc.* **137** (1990) 1772.
7. M. Azuma, K. Hashimoto, M. Hiramoto, M. Watanabe and T. Sakata, *J. Electroanal. Chem.* **260** (1989) 441.
8. D.W. DeWulf, T. Jin and A.J. Bard, *J. Electrochem. Soc.* **136** (1989) 1686.
9. S. Kaneco, K. Iiba, N. Hiei, K. Ohta, T. Mizuno and T. Suzuki, *Electrochim. Acta.* **44** (1999) 4701.
10. B.J. Liaw and Y.Z. Chen, *Appl. Cat. A* **206** (2001) 245.
11. R.L. Cook, R.C. MacDuff and F. Sammells, *J. Electrochem. Soc. Electrochem. Sci. and Tech.* (1988) 3069.
12. R.L. Cook, R.C. MacDuff and F. Sammells, *J. Electrochem. Soc.* **136** (1989) 1982.
13. K. Hara and T. Sakata, *Bull. Chem. Soc. Jpn.* **70** (1997) 571.
14. K. Hara and T. Sakata, *J. Electrochem. Soc.* **144** (1997) 539.
15. N.V. Osterova, V.S. Bagotzky, S.F. Guizhevsky and Yu.M. Serov, *J. Electroanal. Chem.* **453** (1998) 239.
16. T. Mizukawa, K. Tsuge, H. Nakajima and K. Tanaka, *Angew. Chem., Int. Ed. Engl.* **111** (1999) 373.
17. H. Kaune, PhD thesis, Oldenburg, Germany (1994).
18. D.A. Tryk and A. Fujishima, 'Interface', The Electrochemical Society (Spring 2001), p. 32.